**Supporting Information**

# Vesicle-like Assemblies of Ligand-Stabilized Nanoparticles with Controllable Membrane Composition and Properties

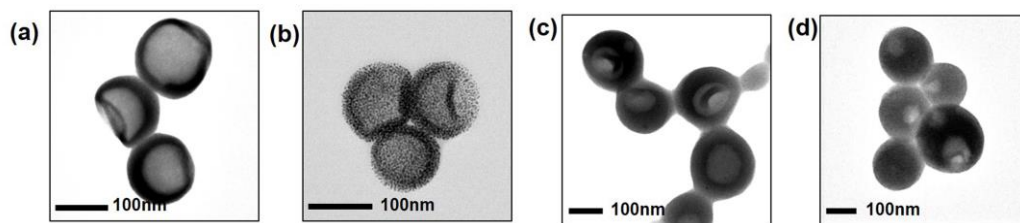*Ji-eun Park, Myungjoo Seo, Eunseon Jang, Haein Kim, Jun Soo Kim,\* and So-Jung Park\**

Department of Chemistry and Nano Science, Ewha Womans University, 52 Ewhayeodae-gil,

Seodaemun-gu, Seoul, 03760, Korea

Email: jkim@ewha.ac.kr, sojungpark@ewha.ac.kr

**Table of Contents**

# 1. Supporting experimental data

**Fig S1**. Additional TEM images of nanoparticle assemblies formed from (a) Au-MUL, (b) Au-MUL80, (c) Au-MUL60, and (d) Au-MUL50. The initial concentration of gold nanoparticles was 1.0 µM for all samples.
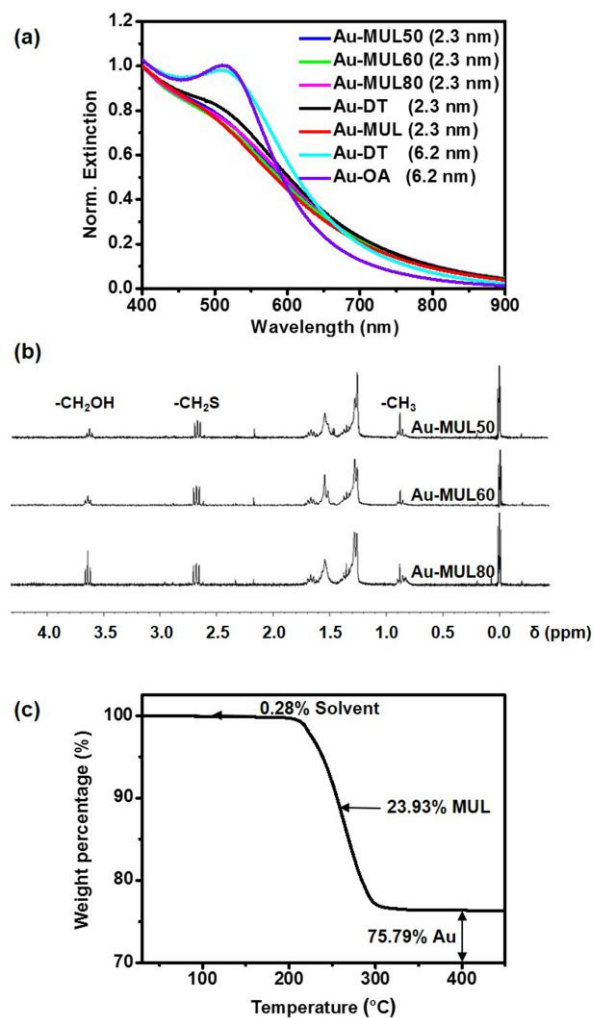
**Fig S2**. (a) UV-Vis extinction spectra of various types of nanoparticles used in this study. (b) Representative $^1$H NMR spectra (CDCl$_3$, 300 MHz) of ligands after iodine treatment for Au-MUL50, Au-MUL60, and Au-MUL80. $^1$H NMR (300 MHz, CDCl$_3$, δ): 3.64 (t, 2H, CH$_2$OH), and 2.70 (t, 2H; CH$_2$S). (c) TGA data of Au-MUL.
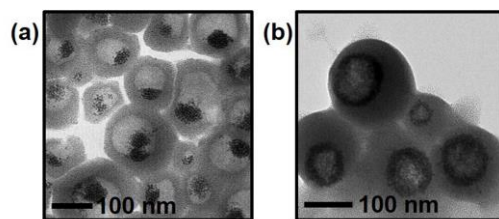
**Fig S3.** (a) TEM images of co-assemblies formed from 2.3 nm Au-MUL and 6.2 nm Au-DT (b) TEM images of co-assemblies formed from 2.3 nm Au-MUL and 6.2 nm Au-OA.
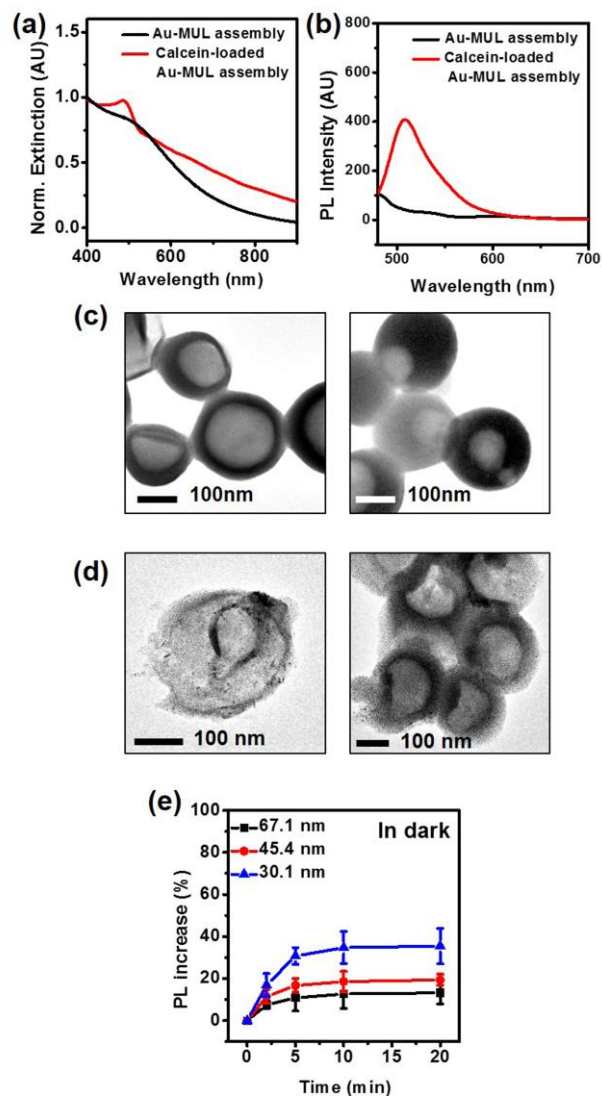
**Fig S4**. (a) UV-Vis and (b) photoluminescence (PL) spectra of Au-MUL assemblies (black) and calcein-loaded Au-MUL assemblies (red). TEM images of nanoparticle assemblies (membrane thickness: 30.1 ± 13.6 nm (left) and 67.1 ± 19.4 nm (right)) (c) before and (d) after 20 min laser irradiation. (e) PL intensity increase over time at 512 nm (excitation wavelength: 450 nm) for Au-MUL assemblies kept in dark, showing that the spontaneous release of dyes also depend on the membrane thickness and the PL intensity plateaued at about 10 min. Therefore, laser-induced dye release experiments were carried out after incubating the solution in dark for 20 min, at which point the spontaneous release appears to stop.
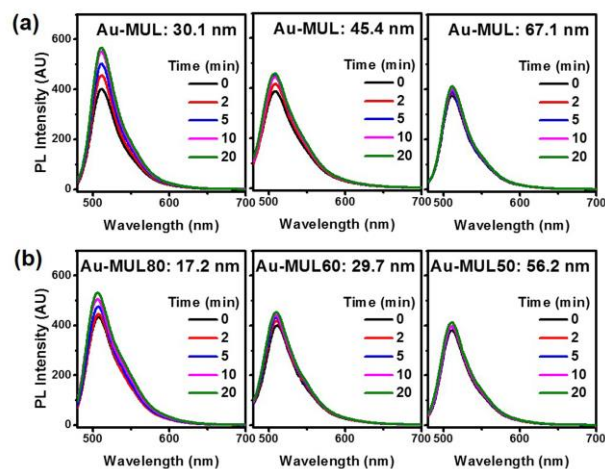
**Fig S5.** Typical PL spectra used to construct light-induced dye release profiles for (a) Au-MUL assemblies with different membrane thickness (30.1 ± 13.6 nm (left), 45.5 ± 10.6 nm (middle), and 67.1 ± 19.4 nm (right)) and (b) nanoparticle assemblies with MUL/DT mixed ligands (Au-MUL80 (left), Au-MUL60 (middle), and Au-MUL50 (right)).

## 2. Details of simulation models and supporting simulation data

Our coarse-grained simulation models were constructed based on three physical parameters: the size and bond lengths of gold nanoparticles and ligands, the ligand density grafted onto a gold nanoparticle, and the ligand flexibility. A gold nanoparticle is modelled as a single sphere with diameter of 6.47σ, where σ is a unit of length and corresponds to σ = 0.355 nm in our model, and marked as a type A as shown in Figure 3a of the main text. The size of a gold nanoparticle was chosen to mimic the size of 2.3 nm estimated in the experiment. As for MUL and DT ligands, three backbone units are lumped into a single interaction site and each ligand is modelled as a chain of five interaction sites. Total 116 ligands are grafted onto a single spherical gold particle, such that the thiol footprint is fixed at 14.5 Å$^2$ following our experimental estimation by the thermogravimetric analysis (TGA) (Figure S2c).

Grafting sites (-S-CH$_2$-CH$_2$-; a type B) of ligands and hydrophilic terminal sites (-CH$_2$-CH$_2$-OH; a type E) are modelled as purely repulsive spheres with diameter of 1σ, and interact with all types of interaction sites (types of B, C, D, and E) through a repulsive part of Lennard-Jones (LJ) potential energy of

$$U_{rep} = \begin{cases} 4\epsilon_r \left[ \left(\frac{\sigma}{r}\right)^{12} - \left(\frac{\sigma}{r}\right)^6 \right] + \epsilon_r & 0 < r < 2^{1/6}\sigma \\ 0 & \text{elsewhere} \end{cases} \tag{1}$$

where $\epsilon_r = 1k_B T$. Middle backbone sites (-CH$_2$-CH$_2$-CH$_2$-; a type C) and terminal groups (-CH$_2$-CH$_2$-CH$_3$; a type D) are hydrophobic and modelled as spheres with diameter of 1σ that interact attractively with interaction sites of either types of C or D through  the LJ potential energy of

$$U_{att} = \begin{cases} 4\epsilon_a \left[ \left(\frac{\sigma}{r}\right)^{12} - \left(\frac{\sigma}{r}\right)^6 \right] & 0 < r < 2.5\sigma \\ 0 & \text{elsewhere} \end{cases} \qquad (2)$$

where $\epsilon_a = 1.7 k_B T$. The potential is truncated and shifted at a cutoff distance of $2.5\sigma$. For $\epsilon_a <$ $1.7 k_B T$, the Au NPs with $f_E$ = 100% do not form a single cluster in the MD simulations. For larger value of $\epsilon_a$, for instance, of $2.0 k_B T$ the attraction between interactions sites of C and D is so strong that a linearly connected, infinitely long cluster is formed throughout the periodic simulation box even at $f_E$ = 0%. The interaction between Au NPs (a type A) is assumed purely repulsive by

$$U_{rep} = \begin{cases} 4\epsilon_r \left[ \left(\frac{\sigma}{r-r_0}\right)^{12} - \left(\frac{\sigma}{r-r_0}\right)^6 \right] + \epsilon_r & 0 < r < 2^{1/6}\sigma \\ 0 & \text{elsewhere} \end{cases} , \qquad (3)$$

where $\epsilon_r = 1 k_B T$ and $r_0 = 5.47\sigma$. The interaction of an Au NP (a type A) with other ligand interaction sites (types B, C, D, and E) is also assumed purely repulsive with the same interaction potential of Eq.(3) but with different $r_0 = 3.74\sigma$.

The MUL and DT ligands are modelled as polymer chains of -B-C-C-C-E and -B-C-C-C-D, respectively, for which the five interactions sites are bonded using a combination of a finite extension linear elastic (FENE) potential energy

$$U_{fene} = -\frac{1}{2} k_f R_f^2 \ln \left[ 1 - \left(\frac{r}{R_f}\right)^2 \right] \qquad (4)$$

and a repulsive LJ potential energy described in Eq.(1), where $k_f = 30 k_B T/\sigma^2$ and $R_f = 1.5\sigma$. These parameters are chosen to ensure that the chains do not pass through each other.

The flexibility of each ligand chain is set by a harmonic restraint on each angle formed by three consecutive interaction sites
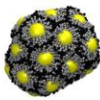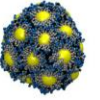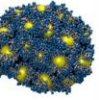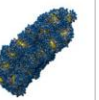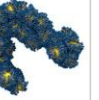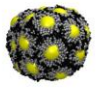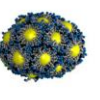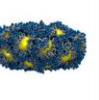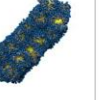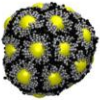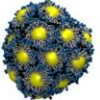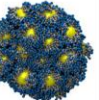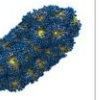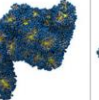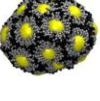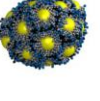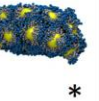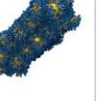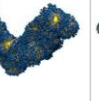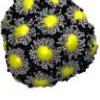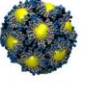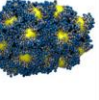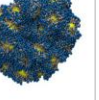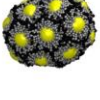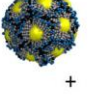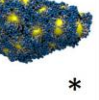
$$U_{angle} = \frac{1}{2}k_{angle}(\theta - \theta_0)^2,$$

where $\theta$ is the angle between two consecutive bond vectors connecting three interaction sites, $\theta_0 = 0$, and $k_{angle} = 2k_BT/\text{rad}^2$. The persistence length is estimated as 9.2 Å, slightly longer than that of polyethylene (6.5 Å). However, the bond angle at the grafting site formed by model particles A-B-C is unrestrained.

Grafting sites are permanently bonded to a gold nanoparticle through a harmonic bond potential energy

$$U_{har} = \frac{1}{2}k_h(r - b_h)^2$$

where $k_h = 90k_BT/\sigma^2$ and $b_h = 3.73\sigma$ to ensure the strong binding of all the ligands on the surface of a gold nanoparticle.

**Fig S6.** Self-assembled structures with different ligand compositions, obtained from three independent simulations. The structures presented in set 1 are the same as those given in Figure 3b. For those marked with * symbol, twice longer simulations (with duration of $6\times10^7$ MD steps) were run to obtain a single cluster of nanoparticles. For the snapshots marked with + symbol, a single cluster formation was not completed after simulation duration of $3\times10^7$ MD steps and only the largest cluster is shown in the figure.

**Table S1**. Average number of neighboring gold nanoparticles around each single gold nanoparticle. $\langle N_1 \rangle$ is the average number with a cutoff distance of $10.0\sigma$ and $\langle N_2 \rangle$ is that with a cutoff distance of $13.0\sigma$. These cutoff distances were chosen from RDF in Figure 4a to include only the first peak and both the first and second peaks, respectively. The values of $\langle N_1 \rangle$, thus, count the number of neighbors with anisotropic edge-to-edge binding, those of $\langle N_2 \rangle$ count the number of all binding neighbors, and those of $\langle N_2 \rangle - \langle N_1 \rangle$ represent the number of neighbors with isotropic binding. The value in the parenthesis indicates the standard deviation from three independent simulations.

| | $f_E$ = 0% | $f_E$ = 20% | $f_E$ = 40% | $f_E$ = 60% | $f_E$ = 80% | $f_E$ = 100% |
|---|---|---|---|---|---|---|
| | spherical | spherical /oblate | oblate | prolate | planar /linear | linear /branched |
| $\langle N_1 \rangle$ | 0.57 (0.09) | 0.54 (0.17) | 1.88 (0.09) | 2.35 (0.09) | 2.32 (0.03) | 1.98 (0.03) |
| $\langle N_2 \rangle$ | 7.48 (0.06) | 7.04 (0.69) | 6.67 (0.16) | 5.90 (0.18) | 3.90 (0.17) | 2.00 (0.00) |
| $\langle N_2 \rangle - \langle N_1 \rangle$ | 6.91 (0.11) | 6.5 (0.71) | 4.79 (0.18) | 3.55 (0.20) | 1.58 (0.17) | 0.02 (0.03) |